CONF-901023--8

SAND--90-1770C

DE91 001336

CHARACTERIZATION OF SEMICONDUCTOR SURFACE-EMITTING LASER WAFERS

P. L. Gourley, G. A. Vawter, T. M. Brennan, and B. E. Hammons
Sandia National Laboratories

Albuquerque, NM 87185

The development of epitaxial semiconductor surface-emitting lasers has begun in recent years. These lasers are ultra-short (few μm) Fabry-Perot resonators comprising epitaxial multilayer semiconductor mirrors and quantum well active regions. The resonators are single crystals grown along the lasing axis by molecular beam epitaxy (MBE) or chemical vapor deposition (CVD). They offer significant advances over conventional cleaved, edge-emitting lasers for creating lasers with single elements or 2 dimensional arrays, low beam divergence, engineered active regions, single longitudinal modes, and improved temperature characteristics. To realize the high potential of these new laser structures, techniques for characterizing the laser wafer after growth and between fabrication steps must be developed. In this paper we discuss several optical techniques that we have developed for this emerging surface-emitting laser technology.

INTRODUCTION

The semiconductor laser was first demonstrated in 1962 and has steadily developed to the present. In these lasers the photons travel laterally in the wafer plane, with feedback provided by crystal facets or lateral modulation of the wafer refractive index. These lasers have shown remarkable power efficiencies, compact size, and are beginning to find widespread application. Despite these advances, the in-plane semiconductor laser has been limited in the quality of the optical beam because of wide divergence and astigmatism. Recently we have demonstrated a fundamentally new kind of semiconductor laser which emits a low divergence, circular beam vertically out of the wafer plane (1). These lasers are single crystal Fabry-Perot resonators comprising semiconductor mirrors and quantum well active regions precisely grown layer-by-layer using either molecular beam epitaxy or chemical vapor deposition growth techniques. Because the mirrors are highly reflective, up to 99.9%, the active length can be as short as a single quantum well the order of 100 Å (2). Such ultrashort cavities give lasing operation on a single longitudinal mode. Because the lasing occurs along the growth direction, the active region can be artificially structured layer by layer to implement periodic gain (3). Further, the laser aperature is now independent of the active region layer geometry and can be artificially controlled to create 2-dimensional coherent laser arrays for the first time (4). These lasers are ideally suited to the use of strained-layer quantum wells (5). The layer strain provides a fundamental modification of the valence bands which enhances the laser performance.

To realize the enormous potential of these new laser structures, new methods must be developed to characterize the laser wafer after growth and between fabrication steps of the device processing sequence. In this paper, several new optical characterization techniques will be discussed. Most of these techniques utilize a laser microscope which allows various laser sources to be optically coupled

DISTRIBUTION OF THIS DOCUMENT IS UNLIMITED

MASTER

(on a microscopic scale) to the wafer while simultaneously allowing spontaneous and stimulated light to be collected and analyzed.

BASIC CONCEPTS OF SEMICONDUCTOR QUARTER-WAVE STRUCTURES

Semiconductor Mirrors

Most of the structures to be characterized fall into a broader classification of quarter-wave structures. All of these structures comprise epitaxial multilayers of semiconductor materials. Alternating layers of materials with high and low refractive indices are built up in periodic growth process. Each layer in the multilayer is chosen to be one quarter wave of a particular wavelength. The optical thickness of each layer is the wavelength divided by 4n where n is the refractive index of the layer. The multilayers produces a Bragg reflection condition at wavelength $\lambda_o=2(n_H d_H + n_L d_L)$ where n and d are the layer refractive index and thickness, respectively, and H and L refers high and low index of refraction for the two materials. The width of the high reflectance zone is given by $\Delta\lambda/\lambda_o \approx 4(n_H - n_L)/\pi(n_H+n_L)$. The maximum reflectance of a mulilayer on a substrate with index n_s is given by $R_m=[(1-n^*)/(1+n^*)]^2$ where n^* is an effective index of the multilayer as a whole given by $n^*=(n_H/n_L)^{2N}(n_H^2/n_s)$. For large n^* the reflectance $R_m \approx 1-4/n^*$. Thus, when sufficient number of layer periods are grown, the multilayer serves as a highly reflecting mirror when light is directed to the wafer surface. Reflections from successive interfaces are coherent and build up a large reflected wave. For typical semiconductor pairs like GaAs and AlAs, which differ in refractive index by about 20%, the mirror reflectance can approach 99.9% if 20 layer periods are grown.

Semiconductor Fabry-Perot Resonators

In the surface-emitting laser, a bottom mirror is grown followed by a spacer layer (or active region), followed by a top mirror. The total thickness of all the grown layers is about 5 to 10 microns. The mirrors are typically 2 to 3 microns each. In the active region, quantum wells are grown to provide gain. The resulting structure is a single crystal Fabry-Perot resonator. The mirror layer thicknesses are chosen to reflect the light emitted from the quantum wells. When emitted, such light is trapped by multiple reflections between the mirrors. With high carrier densities in the quantum well, gain is

present and the optical wave intensifies during its transit between mirrors. The resonator will build up optical waves only when a wave remains in phase after a round trip between mirrors. This phase condition restricts the lasing process to occur only at the resonant frequencies of the optical resonator. The longitudinal mode energies of resonator are given by $\epsilon_m = \hbar k_m c$ where c is the speed of light, and $k_m = 2\pi/\lambda_m$ is the mode wavevector, and λ_m is the mode wavelength. The wavevector is related to the structural parameters by $k_m = (2\pi m - \phi_1 - \phi_2) n_m / 2\ell$ where ℓ is the active region thickness, m is an integer, the ϕ_i are the optical phases of the two mirrors, and n_m is the effective index of the active region at mode energy ϵ_m. The optical phase of the mirror within the high reflectance zone is approximated by $\phi_i \approx \phi_o + \pi n_m (\epsilon - \epsilon_o)/\epsilon(n_H - n_L)$ where ϕ_o (0 or π) is the phase at $\epsilon_o = hc/\lambda_o$ the energy of zone center The separation of longitudinal modes is $\Delta\epsilon \approx \pi\hbar c/\ell(n_m - \epsilon_m dn/d\epsilon)$ which is typically in the range 50 to 100 meV.

The Fabry-Perot resonator has transmittance given by

$$T = \frac{\gamma}{1 + F\sin^2(\theta/2)} \tag{1}$$

where

$$\gamma = \frac{(1-R_2)(1-R_1)\ e^{-\alpha\ell}}{(1-\sqrt{R_1}\sqrt{R_2}\ e^{-\alpha\ell})^2} \tag{2}$$

and

$$F = \frac{4\sqrt{R_1}\sqrt{R_2}\ e^{-\alpha\ell}}{(1-\sqrt{R_1}\sqrt{R_2}\ e^{-\alpha\ell})^2} \tag{3}$$

and α is the effective absorption coefficient in the active region and θ is the round trip phase change within the resonator. It is given by

$$\theta = \phi_1 + \phi_2 - 2(2\pi n\ell/\lambda) \tag{4}$$

The transmittance T exhibits a maximum when $\theta = m\pi$, where m is an integer, and a minimum halfway between these values of θ. The ratio of the separation of maxima to the width of the maxima is given by the finesse $\pi\sqrt{F}/2$.

Semiconductor Surface-emitting Lasers

When the active region in the Fabry-Perot resonator is capable of producing optical gain, the structure can sustain lasing oscillation. To produce gain, electron-hole pairs are created in the active region by electrical injection. They can also be produced optically by an external light source. This latter method is discussed in the present paper because of usefulness in characterization.

For the case of a quantum well active region the lasing process can be described semi-classically by rate equations for the 2D photon density π and the 2D carrier density σ :

$$\dot{\sigma} = \frac{J}{N_t} - \gamma_e\sigma - \frac{G\pi}{N^*} - \gamma_{sp}\sigma \quad (5)$$

$$\dot{\pi} = (G - \gamma)\pi + \gamma_{sp}N^*\sigma \quad (6)$$

where J is the injection rate of electron-hole pairs into an active region with N_t quantum wells. The γ_{sp} and γ_e are recombination rates for spontaneous emission for the mth longitudinal mode and nonradiative recombination, respectively. The cavity gain rate is $G = \Gamma\nu_g N^* g_q/L$ where Γ is the confinement factor (assumed to be unity in the present analysis) and the group velocity is $\nu_g = c/n_g$ where c is the speed of light and n_g is an effective refractive index. N^* is the effective number of quantum wells participating in the gain process and includes the effects of spatial alignment of the quantum wells with the cavity standing wave. L is the cavity length. The quantity $\gamma = \gamma_m + \gamma_{int}$ is the sum of the cavity loss rates due to mirror loss γ_m and internal losses (absorption and scattering) γ_{int} where $\gamma_m = \nu_g\alpha_m$ and

$\gamma_{int} = \nu_g \alpha_{int}$. The quantity $\alpha_m = (1/L)\ln(1/R_1R_2)$ and the α_{int} is an effective absorption coefficient.

The quantity g_q is the net gain per quantum well. This important quantity determines much of the lasing physics. Although many theories exist to describe it, experimental measurements have not yet verified them. A simple theory gives

$$g_q = \frac{4\pi e^2 M^2 \mu}{ncm^2\omega\hbar^2}[f_c(\omega'\mu/m_c) - f_v(\omega'\mu/m_v)] \tag{7}$$

where n is the refractive index, e and m are the free electron charge and mass, M is a momentum matrix element, and μ is the reduced mass. The quantity $\hbar\omega' = \hbar\omega - E_g$ is the photon energy reduced by the bandgap energy. The f_i are the 2-dimensional fermi distribution functions for the conduction (c) and valence (v) bands. The factor $f_c - f_v$ in Eqn (7) determines most of the essential lasing physics.

Steady state solutions to Eqns (5) and (6) for σ and π indicate that the function $\sigma(J)$ exhibits a linear increase with injection rate J until σ saturates near lasing threshold (6). The function $\pi(J)$ increases linearly with J except at threshold where an abrupt increase occurs. The lasing threshold occurs when the stimulated emission rate $G\pi/N^*$ exceeds the nonradiative recombination rate $\gamma_e\sigma$ at a threshold injection rate J_{th}. Analysis of the solutions for a wide range of values for N^* and mirror loss $\delta = 1 - R_1R_2$ show that lasing will occur if δ is less than a critical mirror loss δ_c which is approximated by $\delta_c \approx 1.5\times10^{-3}N^*$. When δ is very small corresponding to a high reflectance limit, the threshold injection rate is independent of mirror loss and scales directly with the number of quantum wells in the active region.

OPTICAL CHARACTERIZATION

The above descriptions of the semiconductor mirrors, Fabry-Perot resonator, and lasing process define the important characteristics of the surface-emitting laser. The mirrors are characterized by the wavelength, magnitude and phase of the reflectance. The resonator is characterized by the frequencies and sharpness of it resonances. The laser is characterized by the threshold injection rate and output efficiency. These latter two characteristics are primarily dependent on the mirror loss δ and effective gain in the active region. Aside from these are the quality of the materials which comprise the resonator, including the quantum wells.

Reflectance Topography

A very useful technique to assess the quality of quarter-wave structures is reflectance topography which is illustrated in Fig. 1. This technique is particularly useful for assesssing the lateral variation of the mirror reflectance across the wafer. It is the easiest of the techniques and can be done immediately after wafer growth without any sample preparation. The wafer is illuminated with monochromatic incoherent light. Typically a tungsten lamp with a narrow and interference filter corresponding to the design wavelength of the laser is used. The specular light reflected from the wafer is directed to a silicon charge-coupled detector (CCD) camera. The surface image of the wafer is brought to focus on the camera. The result is that regions of high and low reflectance can be mapped directly in the camera image. This image determines the extent of lateral variation in the mirror layer thicknesses. By inserting interference filters corresponding to different wavelengths the exact mirror period can be mapped across the wafer. Reflectance topographs from MBE and MOCVD wafers are shown in Fig. 2. There are significant differences in the lateral wafer variation between the two growth techniques. Rotated MBE substrates usually produce a circular reflectance topograph independent of the wafer shape. Care must be taken to center the beam flux near the center of the wafer, or slightly off center to produce the greatest uniformity of layer thickness. In the case of CVD, the boundaries of the wafer help determine the flow of gas over the wafer. As a consequence, the contours of constant reflectance in the topographs vary according to the shape of the wafer. In Fig. 2 the CVD image shows reflectance contours which conform to the crescent shape of the wafer. Typical layer thickness variations of MBE and CVD wafers are a small as 2%. However, care must be taken to exclude those portions of the wafer with lower reflectivity from subsequent processing.

Reflectance/Transmittance Spectroscopy

Once the lateral variation across the wafer is characterized, a more quantitative measurement of the surface normal reflectance can be performed. If the wafer variation is sufficiently small, standard reflectance spectrometers which sample cm sized areas can be used. If the variation is large, microsampling must be used. The reflectance measurement reveals the position and magnitude of the high reflectance zone. Further, it reveals the resonance frequencies of the resonator which appear as sharp minimum within the high reflectance zone. Typically the resonance frequencies vary across the wafer, but this variation can be as little as 5%. Complementing the reflectance technique is transmittance spectroscopy. This technique usually requires some sample preparation such as substrate removal. Like reflectance, the transmittance provides an accurate measurement of the resonator frequencies and linewidths. Further, it provides a measurement of the transmittance minima. This measurement gives an upper limit on the absolute mirror reflectance. Absolute reflectance is difficult to obtain directly from the reflectance spectra when the mirrors are greater than 99% reflective.

Laser photoexcitation

After initial characterization of the mirrors and resonator by incoherent light, it is useful to employ laser photoexcitation to optically pump the structure to the lasing condition. The experimental setup to accomplish this is shown in Fig. 3. A laser source is

directed via a beamsplitter to an objective lens. Under the objective lens the wafer is placed on an x-y translation stage. For low temperature characterization, the wafer can be cooled in a miniature Joule-Thompson apparatus. The objective lens focusses the laser light to a small, spot of controllable diameter on the wafer. Spontaneous or stimulated light from the wafer is collected through the same objective lens and passed through the beamsplitter. This output light can be directed to a variety of analytical instruments. For simple images of the near field (image corresponding to the wafer plane) the light is directed to an infrared vidicon or charge-coupled detector (CCD) TV camera. The TV camera can be cooled to allow long time exposures, necessary for low intensity images. Alternately the vidicon or CCD camera can be positioned away from the wafer image plane to record the far field intensity distribution. The camera images can be digitized and stored in computer memory for analyzing the spatial distribution of the emitted light. By coupling the light into a spectrometer, the energy distribution of emitted photons can be studied. By coupling the light into a calibrated power meter, absolute intensity measurements can be made.

The laser microscope can be used to test wafers for lasing, assuming that the structure has been properly designed with sufficient mirror reflectivities and active region gain. If the structure is pumped with low irradiance below $\sim 10^3$ W/cm^2 the structure will emit only spontaneous light. This light is quite useful for it reveals most of the resonant frequencies of the laser structure. It is important that the gain spectrum and resonator frequencies are spectrally aligned. If the alignment is good, the emitted spectrum appears in the form of discrete emission frequencies corresponding to the resonator frequencies. If the pump light is increased to $\sim 10^4$W/cm^2, one of these frequencies can support the lasing process with intense, coherent light emitted.

In the optical pumping scheme the choice of pump laser wavelength is critical to maximizing the optical absorption in the active region of the SEL. It is desirable to chose a wavelength absorbed by the active region but not the mirror layers. Beyond this, one usually has the choice of pumping at wavelengths inside or outside of the high reflectance zone of the mirrors. Outside this zone the mirror reflectance is usually low such that more light can reach the active region. Inside this zone, the reflectance is very high except at the longitudinal mode wavelengths. It is desirable to chose a mode wavelength where the active region absorbs strongly. Whether pumping inside or outside of the high reflectance zone, there will be pump light reflected, absorbed in the mirrors, or transmitted through the SEL structure. The amount of pump light absorbed by the active region will depend on the structure and can vary considerably. It is necessary to calculate the absorbed power or make direct measurements of the reflected and transmitted light. Even with these direct measurements, there is still some uncertainty about the fraction of light absorbed in the mirrors versus the active region. Another choice in the optical pumping is the laser cycle time. Continuous-wave, quasi-cw, cavity-dumped, and mode-locked pulsed lasers all have been used to pump surface-emitting laser structures.

Optical Scattering

Another useful characterization technique is the measurement of optical scatter. Although this technique has long been used to characterize optical surfaces such as metal and dielectric mirrors, its use for semiconductor multilayers is quite new. Recently this

technique has been used to assess differences in optical scattering in semiconductor multilayers due to growth technique and layer composition (7). Elastic optical scattering is primarily determined by the crystalline imperfection of the mirror layers and interfaces. Defects such as interface roughness, surface defects (hillocks and oval defects), dislocations, and compositional uniformity will all contribute to optical scatter. Despite these defects, epitaxial mirrors are expected to exhibit less optical scatter than conventional multilayer mirrors prepared by vacuum deposition. The latter mirrors exhibit a columnar, polycrystalline morphology which limits the perfection of the layers. This limitation is not present in single crystal semiconductor mirrors which are grown epitaxially on semiconductor substrates such that atomic registration is preserved from layer to layer. Since the substrate serves as a template for the growing crystal, the substrate material can influence the perfection of the grown layers.

The optical scatter from semiconductor multilayers can be determined by measuring the bidirectional reflective distribution function (BRDF) (8). An experimental arrangement is shown in Fig. 4. In this measurement, collimated light near λ_o is directed near normal incidence onto the sample. At this wavelength, only the top surface and first few mirror layers are sampled. Light scattered in the plane of incidence is measured as a function of angle from the normal with a small area photodetector. The BRDF is defined as

$$\mathrm{BRDF} = \frac{1}{P_i/A}\,\frac{dP_s/d\omega_s}{A\cos\theta_s} \qquad (1)$$

where P_i is the incident power, A the irradiated area, and dP_s the differential power scattered into differential solid angle ω_s at angle θ_s from the normal in the plane of incidence. The BRDF measurement yields two important characteristics of the scattering multilayer: total scatter and the power spectral density (PSD). The total scatter from the multilayer can be computed from the BRDF by assuming isotropic scattering. The power spectral density can be calculated directly from the BRDF measurements (9). The PSD can be interpreted as the roughness power per unit spatial frequency.

Recently, the BRDF has been measured for semiconductor quarter-wave structures grown by molecular beam epitaxy and by metal-organic chemical vapor deposition (7). The structures comprise quarter-wave layers of AlGaAs/AlAs and GaAs/AlAs. Histograms of total scatter at incident angle of 9° are shown in Fig. 5 for 2 MBE and one MOCVD wafers. The MOCVD technique yielded the lowest possible total scatter 10^{-5} at selected wafer points, which compares favorably to state-of-the-art ring laser gyro optics. MBE grown wafers yielded the most uniform low scattering across the wafer. Most typically, the total scatter from such either MBE or MOCVD multilayers is about 1×10^{-3} and is probably limited by the quality of the substrate. The power spectral density measured over spatial frequencies from 10^{-3} to 10 μm^{-1} was in the range 10 to 30 Å. Applications such as GaAs-based surface-emitting lasers should benefit by improvements in multilayers which reduce optical scatter. This is particularly true for single quantum well lasers. In these lasers the mirror loss $1-R_1R_2$ must be less than 10^{-3}. Thus, scatter from the multilayer mirrors contributes significantly to the mirror loss. Applications such as this one underscore the need for characterizing the scatter in the semiconductor multilayers.

CONCLUSIONS

Epitaxial semiconductor surface-emitting laser are complex structures requiring detailed understanding of mirror, resonator, and active region properties. We have developed several optical techniques for characterizing these properties. Reflectance topography and Reflectance/Transmittance spectroscopy are useful for determining the mirror loss and resonating frequencies. Laser photoexcitation is useful for characterizing the spectral gain, lasing threshold, and power efficiency. Finally, optical scattering is useful for determining optical losses.

ACKNOWLEDGEMENTS

The authors thank C. F. Shaus, L. R. Dawson who have provided us with some of the laser wafers, and J. C. Stover who helped with the optical scattering measurements. This work is supported by the U. S. Department of Energy under contract number DE-AC04-76DP00789.

REFERENCES

1. P. L. Gourley and T. J. Drummond, Appl. Phys. Lett. 50 1225 (1987).

2. J. L. Jewell, K. F. Huang, K. Tai, Y. H. Lee, R. J. Fischer, S. L. McCall, and A. Y. Cho, Appl. Phys. Lett. 55 424 (1989).

3. S. W. Corzine, R. S. Geels, J. W. Scott, R.-H. Yan, and L. A. Coldren, IEEE J. Quantum Electron. 25 1500 (1989). see also, M. Y. A. Raja, S. R. J. Brueck, M Osinski, C. F. Schaus, J. G. McInerney, T. M. Brennan, and B. E. Hammons, paper, IEEE J. Quantum Electron. 25 1513 (1989).

4. H. Yoo, A. Scherer, J. P. Harbison, L. T. Florez, E. G. Paek, B. P. Van der Gaag, J. R. Hayes, A. Von Lehmen, E. Kapon, and Y. Kwon, Appl. Phys. Lett. 56 1198 (1990).

5. P. L. Gourley, S. K. Lyo, T. M. Brennan, B. E. Hammons, C. F. Schaus, and S. Sun, Appl. Phys. Lett. 55 2698 (1989).

6. P. L. Gourley, Appl. Phys. Lett., accepted.

7. P. L. Gourley, L. R. Dawson, T. M. Brennan, B. E. Hammons, J. C. Stover, C. F. Schaus, and S. Sun, submitted to Appl. Phys. Lett.

8. J. C. Stover, Optical Scattering, McGraw-Hill, New York, NY (1990).

9. J. M. Elson and J. M. Bennett, J. Opt. Soc. Am. 69 31 (1979).

DISCLAIMER

This report was prepared as an account of work sponsored by an agency of the United States Government. Neither the United States Government nor any agency thereof, nor any of their employees, makes any warranty, express or implied, or assumes any legal liability or responsibility for the accuracy, completeness, or usefulness of any information, apparatus, product, or process disclosed, or represents that its use would not infringe privately owned rights. Reference herein to any specific commercial product, process, or service by trade name, trademark, manufacturer, or otherwise does not necessarily constitute or imply its endorsement, recommendation, or favoring by the United States Government or any agency thereof. The views and opinions of authors expressed herein do not necessarily state or reflect those of the United States Government or any agency thereof.

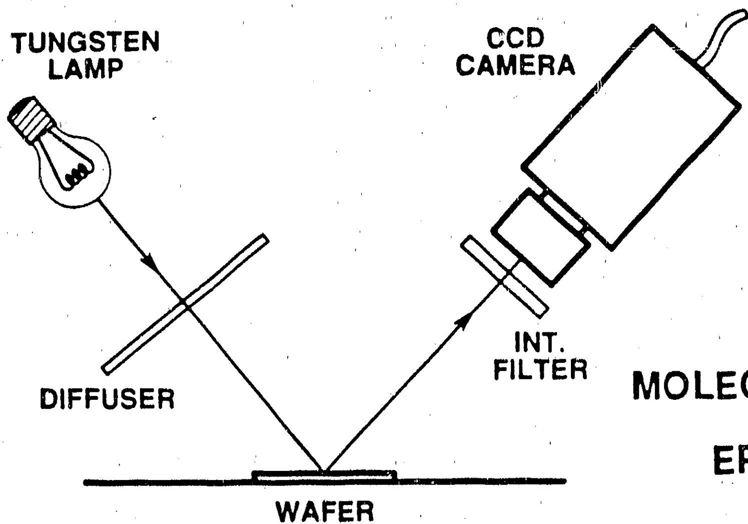

1. Experimental arrangement for obtaining reflectance topographs.

2. Reflectance topographs for MBE and MOCVD laser wafers.

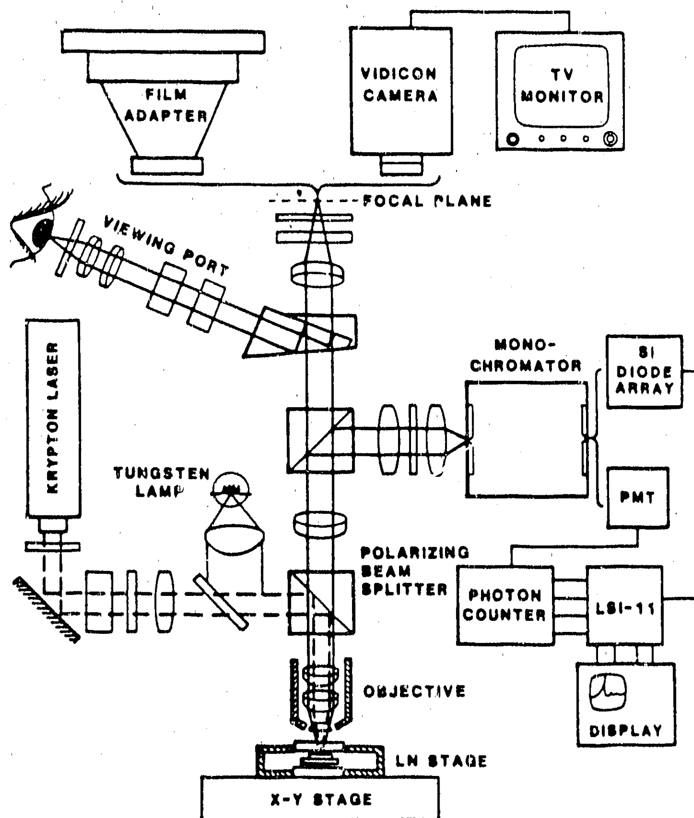

3. Experimental arrangement for photoexcitation studies.

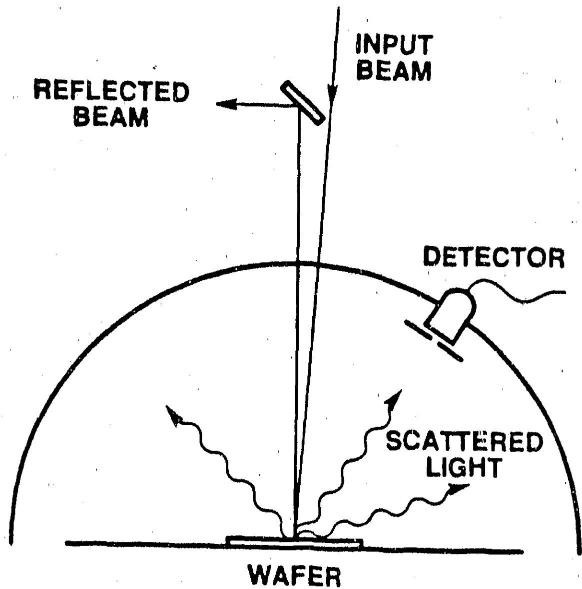

4. Experimental arrangement for optical scatter measurements.

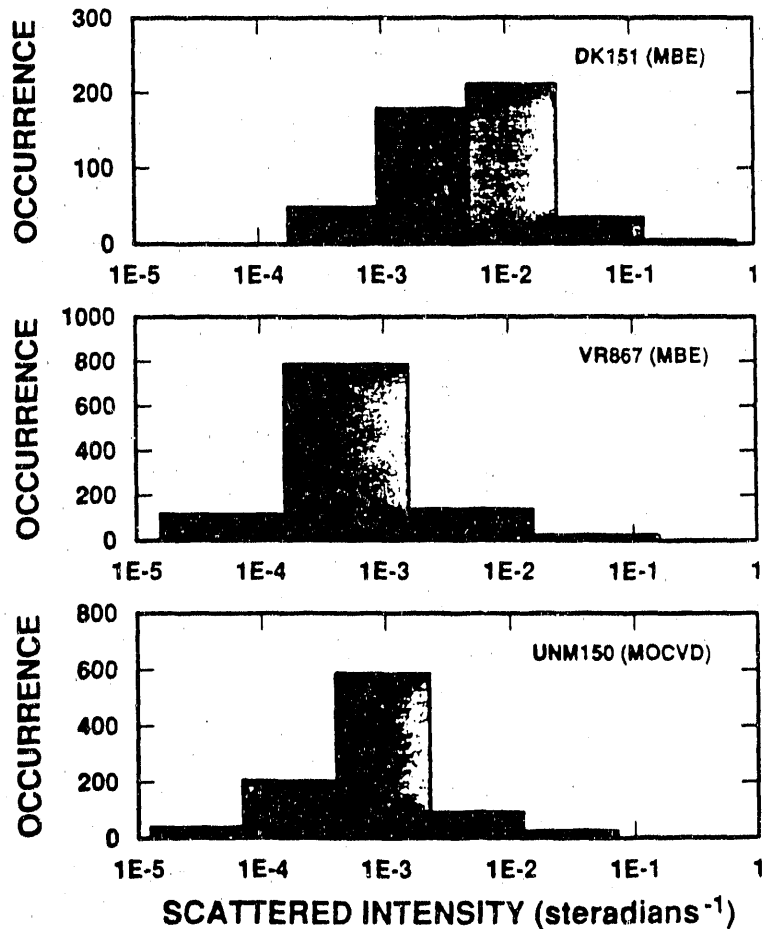

5. Histograms of optical scatter in MBE and MOCVD laser wafers.

END

DATE FILMED

11 / 08 / 90